ELSEVIER

Precision Engineering 27 (2003) 70–86

PRECISION ENGINEERING

www.elsevier.com/locate/precision

Modeling of piezoelectric actuator for compensation and controller design

Jonq-Jer Tzen [a], Shyr-Long Jeng [b], Wei-Hua Chieng [a,*]

[a] *Department of Mechanical Engineering, National Chiao Tung University, 1001 Ta Hsueh Road, Hsinchu 30049, Taiwan, ROC*
[b] *Department of Automation Engineering, Tahwa Institute of Technology, Hsinchu 30049, Taiwan, ROC*

Received 26 June 2001; received in revised form 12 July 2002; accepted 7 August 2002

Abstract

This work proposes a novel method for describing the hysteretic non-linearity of a piezoelectric actuator. The hysteresis behavior of piezoelectric actuators, including the minor loop trajectory and the residual displacement near zero input, are modeled by a set of hysteresis operators, including a gain and an input-dependent lag, as well as the parameter scheduling method. A hysteresis model, using the identified parameters, and containing only the dominant hysteresis operator, is presented herein. Based upon a simplified hysteresis model, tracking is controlled to reduce the non-linear effects in the characteristics of the piezoelectric actuator. A proportional-integral (PI) controller, with inverse model feed-forward, suppresses the tracking error to within ±1% full span range (FSR) of the actuator, noticeably improving the tracking performance of the piezoelectric actuator.

Keywords: Piezoelectric actuator; Hysteresis model; Inverse model compensation

1. Introduction

Piezoelectric ceramics are effective actuation elements in numerous applications that require rapid response and/or ultra-high motion resolution. These applications include optical fiber alignment, mask alignment, scanning by a scanning electron microscope, high precision machining, and the focusing and tracking of a hard disk drive [1]. However, the hysteresis non-linearity between input voltage and output displacement yields a rate-independent lag and residual displacement near zero input, significantly reducing the precision of the actuators.

Hysteresis is an input/output non-linearity with effects of non-local memory. That is, the output of the system depends not only on the instantaneous input but also on the history of its operation. Some papers have proposed the hysteresis model of piezoelectric ceramics, ferromagnetic materials and shape memory alloys. One approach to modeling hysteresis non-linearity, based upon the physical properties of material, is constitutive modeling, as applied in the Jiles–Atherton model for ferromagnetic hysteresis [2]. Alternate approaches are based upon mathematical and logical approximation of the input–output behavior of the material, as, for example, in the Preisach model [3,4], the Duhem model [5], the Maxwell slip model [6], and the constant phase lag approximation [7]. Notably, directly modeling the hysteresis of piezoelectric actuators constitutively, as in the Jiles–Atherton approach for ferromagnetic materials, is difficult, because of the lack of mathematical modeling of the polarization of piezoelectric materials [2]. Consequently, more available models can be established by taking the phenomenological approach.

Several methods exist to reduce the hysteresis non-linearity of the piezoelectric actuator. According to the linear mapping between the driving charge and displacement of the piezoelectric actuator, the charge-driven technique proposed by Newcomb and Flinn [8], although complicated in hardware realization, is an effective method. Employing the Preisach model to compensate for the tracking error of piezoelectric actuators, Ge and Jouaneh [9] proposed a model-based feed-forward compensator. Similarly, Choi et al. [10] presented another version of feed-forward compensation for a piezoelectric actuator that was based upon the Maxwell slip model. Jurgen and Hartmut developed a model-based cascaded compensator that used parallel compensation [11]. Finally, Cru-Hernandez and Hayward [7] recognized the hysteresis non-linearity as a constant phase lag, and thus employed a phase-lead compensator that provides a constant leading phase over a given frequency range. Based

* Corresponding author. Tel.: +886-35-712-121; fax: +886-35-720-634.
E-mail address: whc@cc.nctu.edu.tw (W.-H. Chieng).

0141-6359/02/$ – see front matter © 2002 Elsevier Science Inc. All rights reserved.
PII: S0141-6359(02)00183-6

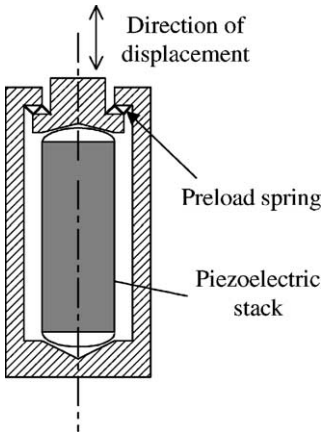

Fig. 1. Preloaded piezoelectric actuator (Burleigh PZL-015, specification listed in Table 1).

upon the various hysteresis models, their work addressed the development of compensation.

This study presents a new hysteresis model that fully encompasses the characteristics of hysteresis non-linearity of piezoelectric actuators. The hysteresis model is based upon a series of hysteresis operators. Each hysteresis operator includes a pair of gain and input-dependent lags, which control the non-linear mapping between input voltage and output displacement. Moreover, a parametric scheduling method, which resets the lag terms of the hysteresis operators when the direction of the input voltage changes, is introduced. A set of memory stacks provided in our parametric scheduling procedure contains the past input and output extremes and thus approximates the non-local memory effect of the hysteresis. By identifying model parameters, when various input voltage waveforms are provided, the simulation completely confirms the experimental results. The proposed model includes all the main features of hysteresis non-linearity, including the major and minor loop behaviors of the piezoelectric actuator. The dominant hysteresis operator can be easily determined from the identified parameters. Without loss of accuracy, the simplified model including only one dominant hysteresis operator is implemented in tracking control for real-time applications.

2. Piezoelectric actuator model

Fig. 1 schematically depicts a preloaded piezoelectric actuator, the Burleigh PZL-015 Low Voltage PZT Pusher [12], which is comprised of a piezoelectric stack and a preload spring. A piezoelectric material stack is formed by stacking many thin plates of piezoelectric material along their axes of polarization with opposite polarization directions between adjacent plates. Two adjacent thin piezoelectric plates share the same electrodes, and are thus connected mechanically in series but electrically in parallel. Moreover, the preload spring prevents the piezoelectric stack from improper bending and stretching motions that may damage it [6,12–14].

Table 1
The specifications of the Burleigh's piezoelectric actuator used in our experiments (from Burleigh instruction manual)

Model number	PZL-015
Material	Lead zirconate titanate (PZT)
Type	Preloaded stack actuator with housing
Dimension	Piezo stack: rectangular disk, 4 mm × 5 mm, 0.25 mm thickness PZT plate, total stack length: 20 mm Housing: ∅ 12.7 mm, length 33.8 mm
Maximum voltage (V)	100
Motion for 0–100 V (μm)	10
Frequency response (kHz)	3.5
Non-linearity (%)	4
Hysteresis (%)	15
Creep (drift)	Increasing voltage: 1–2% in 20–30 s Decreasing voltage: 7–8% in 60–80 s

Table 1 presents the specifications of the commercial piezoelectric actuator used in the experiment.

The hysteresis non-linearity of the actuator is modeled by first dividing the dynamics of the whole structure into linear and non-linear parts, in cascade form, as illustrated in Fig. 2. The mechanical part of this actuator and the linear terms of the piezoelectric stack are considered to be second order linear dynamic. The proposed model of the piezoelectric actuator combines the second order dynamics with the cascaded hysteresis non-linearity for the piezoelectric actuator. Let V_0 and L_0 be the original applied voltage and original length of the piezoelectric actuator, respectively. The mathematical expression for the cascaded model is,

$$\ddot{x} + 2\xi\varpi_n\dot{x} + \omega_n^2 = k\varpi_n^2(F_{ext} + L(V, V_0, X_0)), \quad (1)$$

where ξ, ϖ_n are the damping ratio and the natural frequency of linear dynamics, respectively, V the applied voltage, F_{ext} denotes the normalized external force exerted on the actuator, and $L(\cdot)$ denotes the cascaded non-linear part of the hysteresis non-linearity in terms of its displacement. Fig. 3 presents the Bode diagram of the approximated second order linear dynamics of the actuator connected to the amplifier, which are identified from the experimental data.

As shown in Fig. 4, when the actuator operates away from the saturation voltage, its output displacement may be approximated by an exponential curve, according to the rate-independent lag of the piezoelectric actuator observed in the experiments. Exponential functions describe the piezoelectric hysteresis non-linearity segment by segment. Let V be the input voltage, V_{off} and L_{off} represent the previous

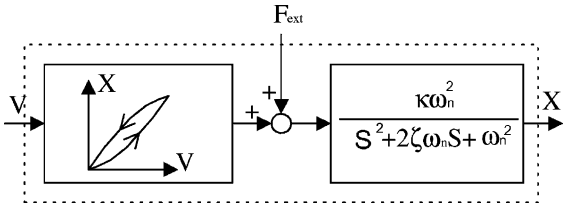

Fig. 2. Cascaded model of piezoelectric actuator.

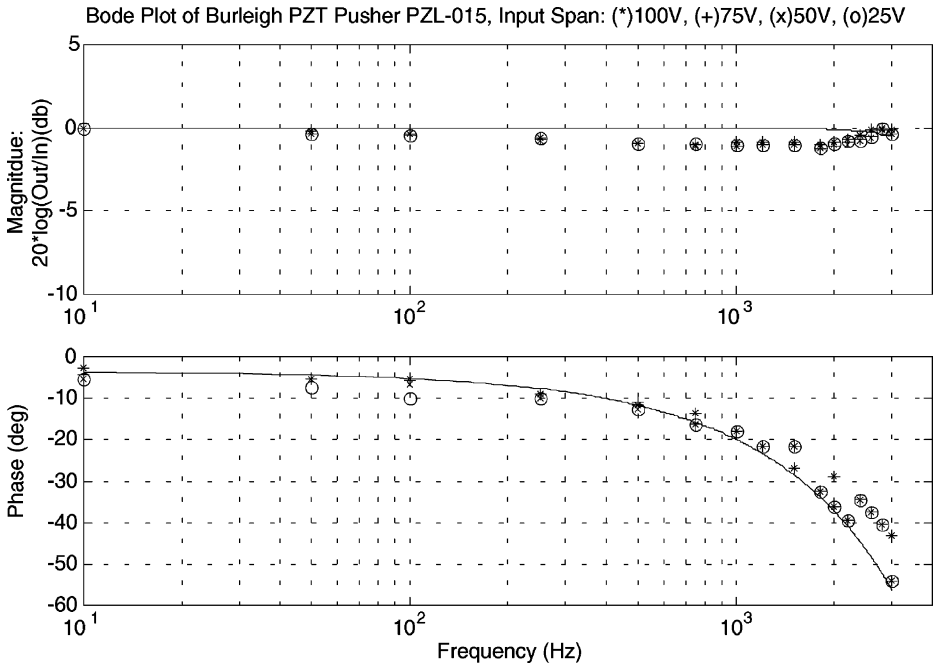

Fig. 3. Measured frequency response of piezoelectric actuator. (The actuator gain is normalized to 1 at 10 Hz.)

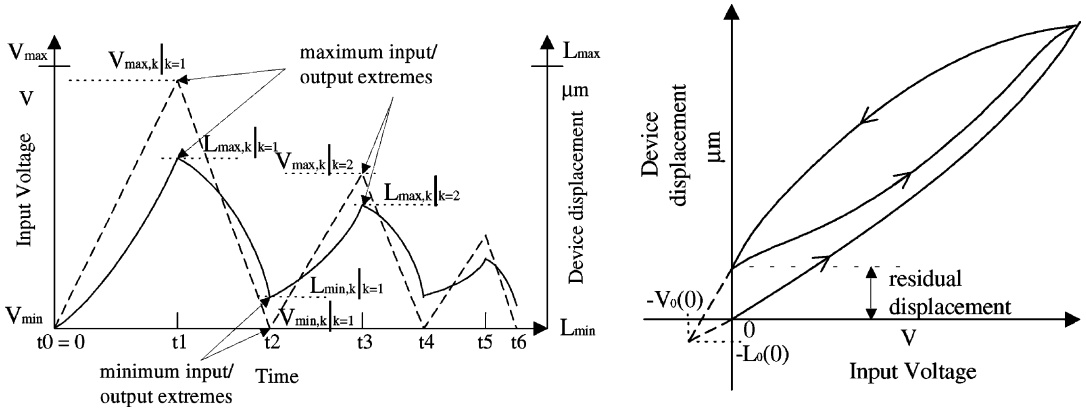

Fig. 4. Definitions of the input/output extremes of our hysteresis model.

extremes of input voltage and actuator displacement, respectively, k_i is the gain of the hysteresis operator, and τ_i represents the input-dependent lag constant of the operator. The output displacement L of the piezoelectric actuator may be expressed as follows:

$$L = \sum_i k_i (1 - \mathrm{e}^{-\tau_i |V - V_{\mathrm{off}}|})(V - V_{\mathrm{off}}) + L_{\mathrm{off}}, \qquad (2)$$

V_{off} and L_{off} must satisfy one of the following conditions:

1. at $t = 0$, $V_{\mathrm{off}} = V_0$, $L_{\mathrm{off}} = L_0$; $V_{\max,k} = V_{\max}$, $L_{\max,k} = L_{\max}$; $V_{\min,k} = V_{\min}$, $L_{\min,k} = L_{\min}$, $k = 0$. V_0 and L_0 represent the initial settings of the corresponding terms. $V_{\min,k}$ and $L_{\min,k}$ ($V_{\max,k}$ and $L_{\max,k}$) represents the minimum (maximum) extremes of input voltage and output displacement in the kth order loop of the hysteresis curve, respectively. $V_{\min}$ and $L_{\min}$ ($V_{\max}$ and $L_{\max}$) represent the minimum (maximum) input voltage and output displacement of the actuator, respectively. The major hysteresis loop has $k = 1$, and $k = 2$ corresponds to the first order minor loop, and so on, as shown in Fig. 4.
2. at t_n,

$$\text{if } \left.\frac{\mathrm{d}V}{\mathrm{d}t}\right|_{t_n^+} \left.\frac{\mathrm{d}V}{\mathrm{d}t}\right|_{t_n^-} < 0, \quad \text{then} \begin{cases} \text{if } \left.\frac{\mathrm{d}V}{\mathrm{d}t}\right|_{t_n^+} < 0, & V_{\min,k} = V_{\mathrm{off}}|_{t_n^-} \text{ and } L_{\min,k} = L_{\mathrm{off}}|_{t_n^-} \\ \text{else,} & V_{\max,k} = V_{\mathrm{off}}|_{t_n^-} \text{ and } L_{\max,k} = L_{\mathrm{off}}|_{t_n^-} \end{cases},$$

$$k = k + 1, \text{ and then } V_{\mathrm{off}} = V|_{t_n}, \; L_{\mathrm{off}} = L|_{t_n},$$

when the direction of the input voltage switches at $t = t_n$, the extremes of input voltage and actuator displacement that occur at that time are substituted for V_{off} and L_{off} in Eq. (2) in the $(k+1)$th loop calculation. $V_{\min,k}$ and $L_{\min,k}$ or $V_{\max,k}$ and $L_{\max,k}$ stores the original extremes of input voltage ($V_{\text{off}}|_{t_n^-}$) and actuator displacement ($L_{\text{off}}|_{t_n^-}$), respectively,

3. at t_i,

   if $V|_{t_i^-} \geq V_{\min,k} > V|_{t_i^+}$,
   then $V_{\text{off}} = V_{\max,k}$ and $L_{\text{off}} = L_{\max,k}$, $\quad k = k - 1$.

4. at t_j,

   if $V|_{t_j^-} \leq V_{\max,k} < V|_{t_j^+}$,
   then $V_{\text{off}} = V_{\min,k}$ and $L_{\text{off}} = L_{\min,k}$, $\quad k = k - 1$.

Comparing the contemporary input voltage with the input extremes of the previous loop reveals whether the trajectory of the actuator has passed through the previous maximum or minimum input voltage extreme. If the input voltage trajectory passes through one of the previous input extremes, the hysteresis will switch from the minor loop back to its ascendant loop, which may be either a minor or a major loop. Otherwise, the hysteresis will continue along the contemporary loop, broadening its span.

3. Parameter scheduling

Eq. (2) describes the non-linear actions of the hysteresis operators. According to the hysteresis operations, Fig. 5 shows the flow chart of the parameter scheduling method to model mathematically hysteresis non-linearity. The parameter scheduling method determines the V_{off} and L_{off} extremes within the hysteresis operator that correspond to the conditions described in the previous section. That is, the

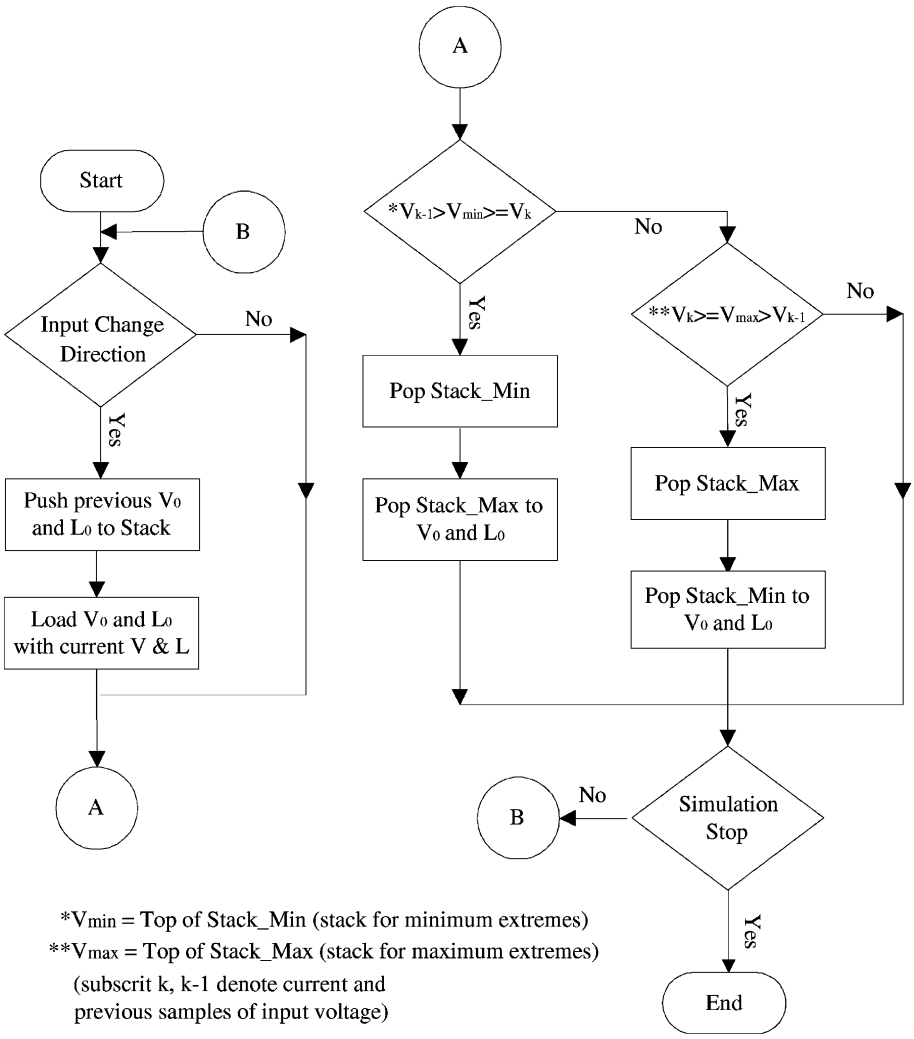

Fig. 5. Flow chart for parameter scheduling. There are two set of stacks for previous extremes storage, $\text{Stack}_{\max}$ is for previous maximum input/output extremes, and $\text{Stack}_{\min}$ is for previous minimum input/output extremes.

parameter-scheduling algorithm realizes the constraints on the values of V_{off} and L_{off} in Eq. (2).

Based on the parameter scheduling, the hysteresis model exhibits the following features:

(1) The hysteresis non-linearity includes linear combinations of hysteresis operators. The features of rate-independence and input-dependent lag dominate the hysteresis.
(2) When the direction of the input switches, parameter scheduling is used to reset both the values of V_{off} and L_{off} into the most recent extremes of input voltage and output displacement, respectively. By the parameter scheduling, the model realizes the central symmetric shape of the hysteresis loop observed in the experiments, and renders the hysteresis behaviors similar to that of non-local memory.
(3) V_{off} and L_{off} were set initially according to experimental observation. The residual displacement of the actuator near zero input voltage may be simulated by setting V in Eq. (2) to zero.
(4) A set of memory stacks was introduced to store both past input and output extremes and thus evaluate correctly the hysteresis loops, including major and minor loops. A comparator was applied to determine the switching point between both minor and major loop. Appropriate switching between the minor and major loops can be obtained to update the V_{off} and L_{off} of Eq. (2) via the comparator and the memory stacks.

4. Gain and lag identification

The conjugate gradient search algorithm [15], a numerical optimization procedure, was modified to obtain a set of precise hysteresis parameters and thereby obtain a good approximation to our hysteresis model via systematic procedures. The identification of parameters in our hysteresis model can be transformed to the problem of finding the actuator gain g as follows:

$$g = \frac{L - L_{\text{off}}}{V - V_{\text{off}}} = \sum_i k_i (1 - \mathrm{e}^{-\tau_i |V - V_{\text{off}}|}) = U^{\mathrm{T}} \tilde{K} - U^{\mathrm{T}} \mathrm{e}^{-\Gamma |V - V_{\text{off}}|} \tilde{K},$$

where

$$U^{\mathrm{T}} = [\,1 \quad 1 \quad \cdots \quad 1 \quad 1\,],$$

$$\tilde{K} = [\,k_1 \quad k_2 \quad \cdots \quad k_n\,]^{\mathrm{T}},$$

$$\Gamma = \mathrm{diag}(\,\tau_1 \quad \tau_2 \quad \cdots \quad \tau_n\,).$$

Let g_0 denote the measured piezoelectric actuator gain. The cost function F integrates (sums) the square error between the measured actuator gain and the modeled actuator gain to minimize the gain error as follows:

$$\begin{aligned} F &= (g_0 - U^{\mathrm{T}} \tilde{K} + U^{\mathrm{T}} \mathrm{e}^{-\Gamma |V - V_{\text{off}}|} \tilde{K})^2 \\ &= g_0^2 + (U^{\mathrm{T}} \tilde{K})^2 + (U^{\mathrm{T}} \mathrm{e}^{-\Gamma |V - V_{\text{off}}|} \tilde{K})^2 \\ &\quad - 2 g_0 U^{\mathrm{T}} \tilde{K} + 2 g_0 (U^{\mathrm{T}} \mathrm{e}^{-\Gamma |V - V_{\text{off}}|} \tilde{K}) \\ &\quad - 2 (U^{\mathrm{T}} \tilde{K})(U^{\mathrm{T}} \mathrm{e}^{-\Gamma |V - V_{\text{off}}|} \tilde{K}). \end{aligned}$$

Then, taking the gradients of the cost function with respect to $\tilde{K}$ and Γ, respectively, yields the following equations:

$$\begin{aligned} \nabla_{\tilde{K}} F &= 2 (U^{\mathrm{T}} \tilde{K}) U + 2 (U^{\mathrm{T}} \mathrm{e}^{-\Gamma |V - V_{\text{off}}|} \tilde{K}) \mathrm{e}^{-\Gamma |V - V_{\text{off}}|} U \\ &\quad - 2 g_0 U + 2 g_0 \mathrm{e}^{-\Gamma |V - V_{\text{off}}|} U \\ &\quad - 2 (U^{\mathrm{T}} \mathrm{e}^{-\Gamma |V - V_{\text{off}}|} \tilde{K}) U - 2 (U^{\mathrm{T}} \tilde{K}) \mathrm{e}^{-\Gamma |V - V_{\text{off}}|} U, \\ \nabla_{\Gamma U} F &= -2 (U^{\mathrm{T}} \mathrm{e}^{-\Gamma |V - V_{\text{off}}|} \tilde{K}) |V - V_{\text{off}}| U^{\mathrm{T}} \\ &\quad \times \mathrm{e}^{-\Gamma |V - V_{\text{off}}|} \tilde{K} - 2 g_0 |V \\ &\quad - V_{\text{off}} |(U^{\mathrm{T}} \mathrm{e}^{-\Gamma |V - V_{\text{off}}|} \tilde{K}) + 2 (U^{\mathrm{T}} \tilde{K}) |V \\ &\quad - V_{\text{off}} |(U^{\mathrm{T}} \mathrm{e}^{-\Gamma |V - V_{\text{off}}|} \tilde{K}). \end{aligned}$$

The gradient for searching algorithm is obtained by the direct sum of the two gradients, $\nabla F = \nabla_{\tilde{K}} F \oplus \nabla_{\Gamma U} F$. The conjugate gradient search algorithm yields a set of hysteresis operators that minimize the error between the estimated and measured outputs.

5. Experimental set-up and parameter identification

Fig. 6 illustrates the experimental design to measure the displacement of the piezoelectric actuator. The Burleigh PZL-015 PZT pusher [13] is used. The nominal displacement of the actuator is around 10 mm when an external voltage of 100 V is applied. Table 1 details this actuator. In the experiments, an HP10705A laser interferometer with a 10 nm resolution and a 3 MHz maximum data update rate measures the actual output displacement of the actuator. The raw digital displacement data are transferred directly to a DSP-based interface card with a 100 kHz reading rate. Another function of the DSP card is to generate various waveforms through a 12-bit D/A converter. The waveforms, assembled via a series of digital data at a 100 kHz D/A rate, are coded in the DSP software. The analog signal is fed into a piezoelectric voltage amplifier, which linearly amplifies it from 0–5 to 0–100 V. The output signal of the voltage amplifier is then used to manipulate the actuator. When the driving voltage of 100 V is input, the maximum displacement of the piezoelectric actuator is around 12 μm.

A low frequency, 1 Hz, input waveform was used in parameter identification to reduce the dynamic effect, which results from the linear dynamics of the actuator. When a 1 Hz triangular wave with amplitude of 100 V was applied to excite the piezoelectric actuator, the laser interferometer with a 1 kHz sampling rate was employed to measure the output displacement. Fig. 7(a) illustrates the input waveform, the measured displacement and the predicted displacement. The errors between the measured and predicted displacements

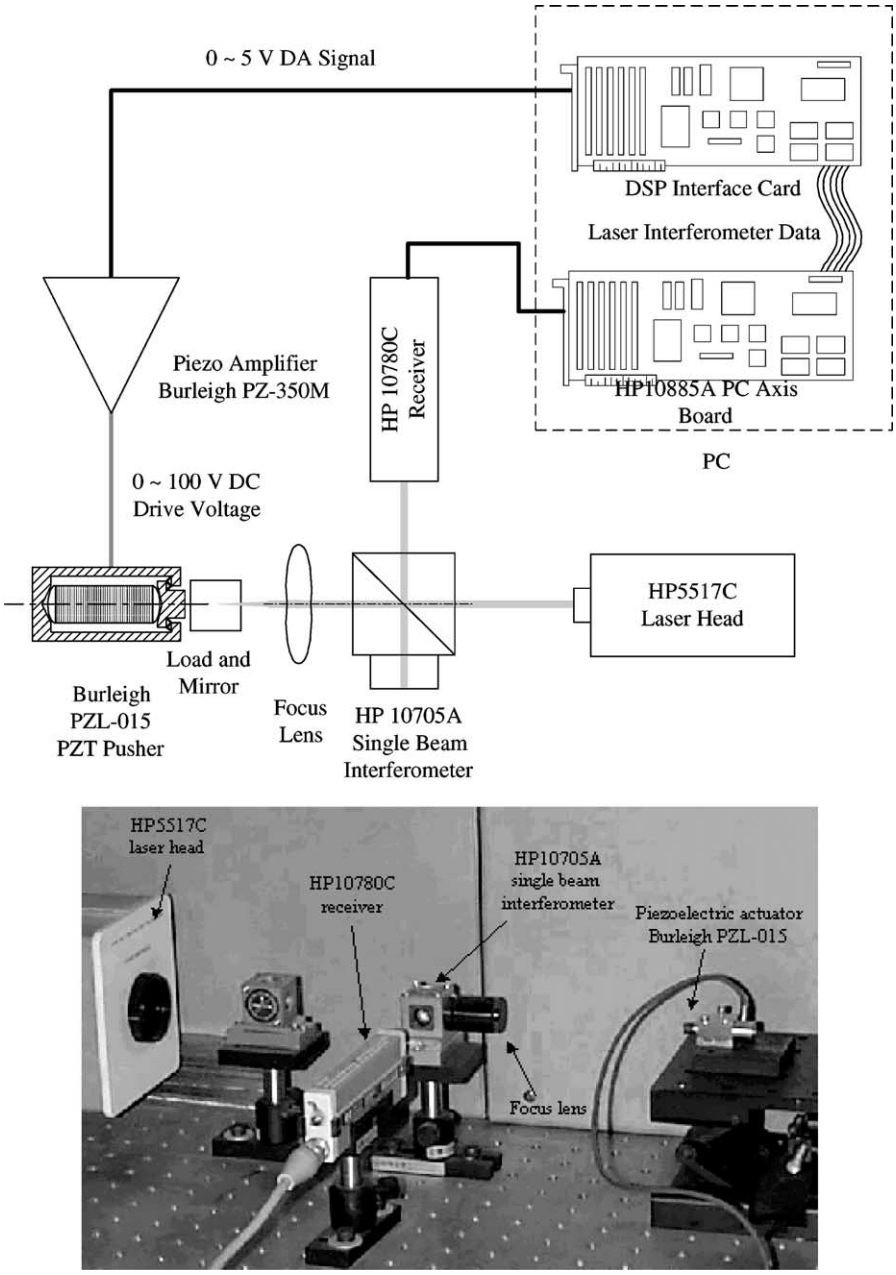

Fig. 6. Experimental set-up.

are also shown. Fig. 7(b) shows the gain (L/V) and gain errors. Table 2 shows the identified parameters.

Four hysteresis operators were employed to model the hysteresis non-linearity of the piezoelectric actuator. The conjugate gradient algorithm with the minimum gain error function was used to identify the model parameters when a series of triangular input waveforms were applied. The same set of gain-lag terms (hysteresis operators) dominates the shapes of the major and minor loops and a series of input waveforms that contains only the major loops suffices to identify parameters.

Table 2
Identified parameters of our hysteresis model

i	k_i (μm/V)	τ_i	$V_{\text{off}}(0)$	$L_{\text{off}}(0)$
1	0.149	1.045	9.0	0.707
2	−0.099	0.500		
3	0.027	0.210		
4[a]	0.077	0.007		

[a] The most dominant hysteresis operator in the model.

A series of experiments on parameters identification was used to observe dependence of model accuracy of the proposed model upon the number of hysteresis operators. These experiments involve many hysteresis models that contain three to eight hysteresis operators. Table 3 lists the maximum modeling errors under various input waveforms and

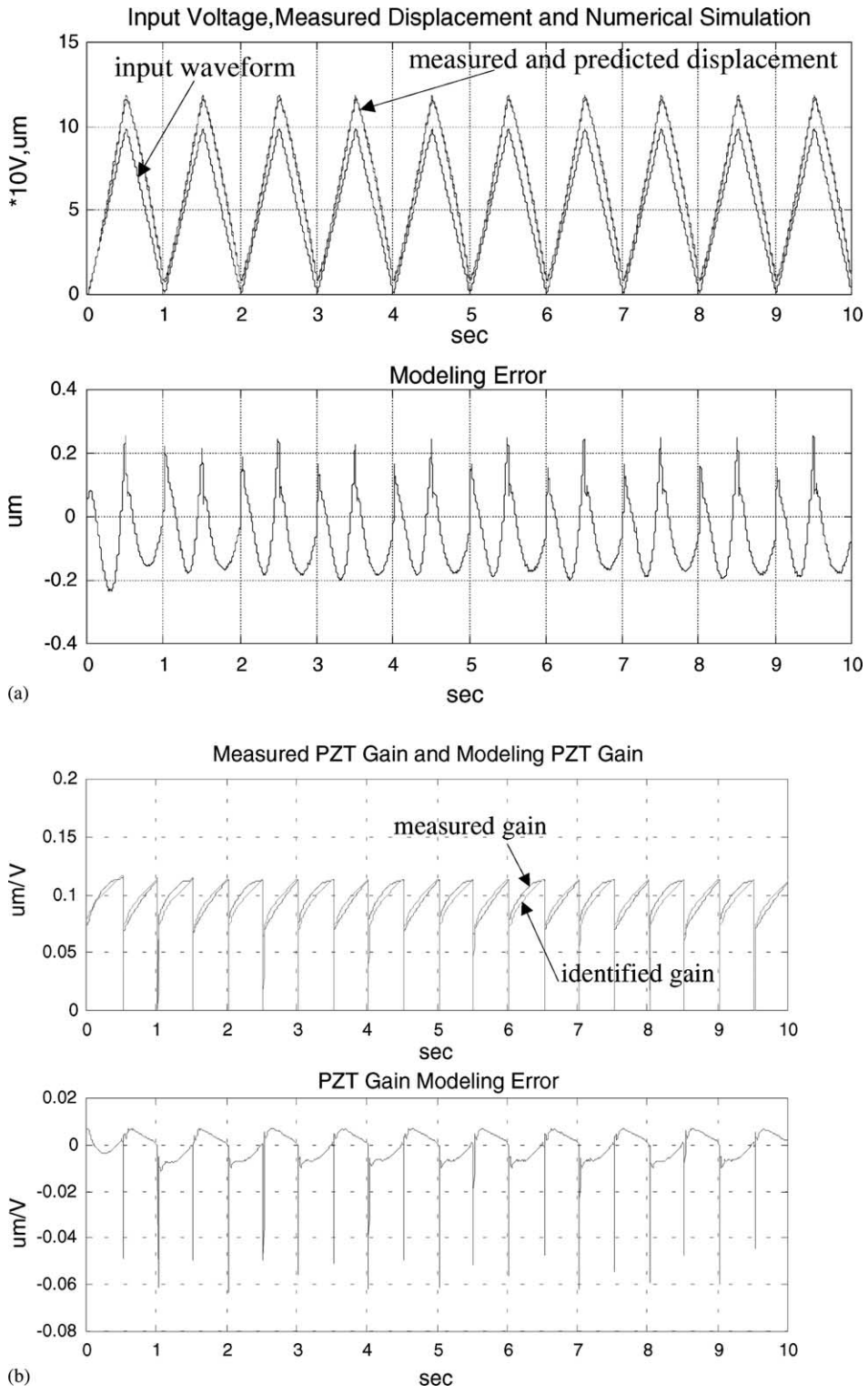

Fig. 7. The results of parameter identification.

hysteresis. A hysteresis model with four or five hysteresis operators clearly suffices to predict the output of the Burleigh PZL-015 piezoelectric actuator. More hysteresis operators that require more computational effort to identify system parameters will not considerably improve the accuracy of the hysteresis model.

According to these hysteresis operator parameters, the hysteresis operator with the most input-dependent lag dominates

Table 3
The dependence of modeling accuracy upon the number of hysteresis operators used in the model

No. of hysteresis operators	Maximum modeling error under different input waveform (μm)				
	Triangular waveform in Fig. 7(a)	Decaying waveform in Fig. 9(a)	Increasing waveform in Fig. 9(b)	Decaying waveform in Fig. 9(c)	Waveform with second order reversal curve in Fig. 9(d)
3	0.44	0.53	0.60	0.58	0.40
4	0.29	0.38	0.38	0.38	0.35
5	0.26	0.37	0.38	0.37	0.35
6	0.27	0.37	0.38	0.38	0.34
7	0.28	0.38	0.38	0.38	0.36
8	0.28	0.38	0.37	0.37	0.35
4[a]	0.29	0.39	0.39	0.38	0.37

[a] The simplified model simplified based on the model with four operators.

the hysteresis non-linearity of the piezoelectric actuator. For example, the fourth hysteresis operator $[k_4, \tau_4] = [0.077, 0.007]$ shown in Table 2 dominates the hysteresis behavior. Consequently, to reduce the computational effect in real-time applications, such as tracking control, the hysteresis model may be simplified as follows:

$$L = (K - k_4\, e^{-\tau_4|V - V_{off}|})(V - V_{off}) + L_{off}, \quad (3)$$

where $K = \sum_i k_i$. Comparing the modeling errors in the second and last rows of Table 3 shows that the simplified hysteresis model with one exponential lag term is as accurate as the unsimplified model. The gain K in Eq. (3) can thus be treated as a hysteresis operator with large exponential lag, τ. Then, the minimum number of hysteresis operators required to model the hysteresis non-linearity is two.

6. Sensitivity of parameter variation

The sensitivity of the proposed hysteresis model to parameter variation can be observed directly from the gradient of the simplified hysteresis model in its parameter space. The gradient vector $\nabla_{[K,K_d,\tau_d]}$ is,

$$\nabla_{[K,K_d,\tau_d]} = \{\bar{K} + e^{-\tau_d|V - V_{off}|}\bar{k}_d + k_d|V - V_{off}|e^{-\tau_d|V - V_{off}|}\bar{\tau}_d\}(V - V_{off}).$$

The base vector $[\ \bar{K} \quad \bar{k}_d \quad \bar{\tau}_d\ ]^T$ spans the parameter space of the simplified hysteresis operator. The subscript 'd' indicates 'dominant.' From the above formulation, the parameter variation can be predicted to be amplified by $(V - V_{off})$ and the parameter to which the model is most sensitive is the sum of the gains of all hysteresis operators. Fig. 8 plots the sensitivity to parameter variation.

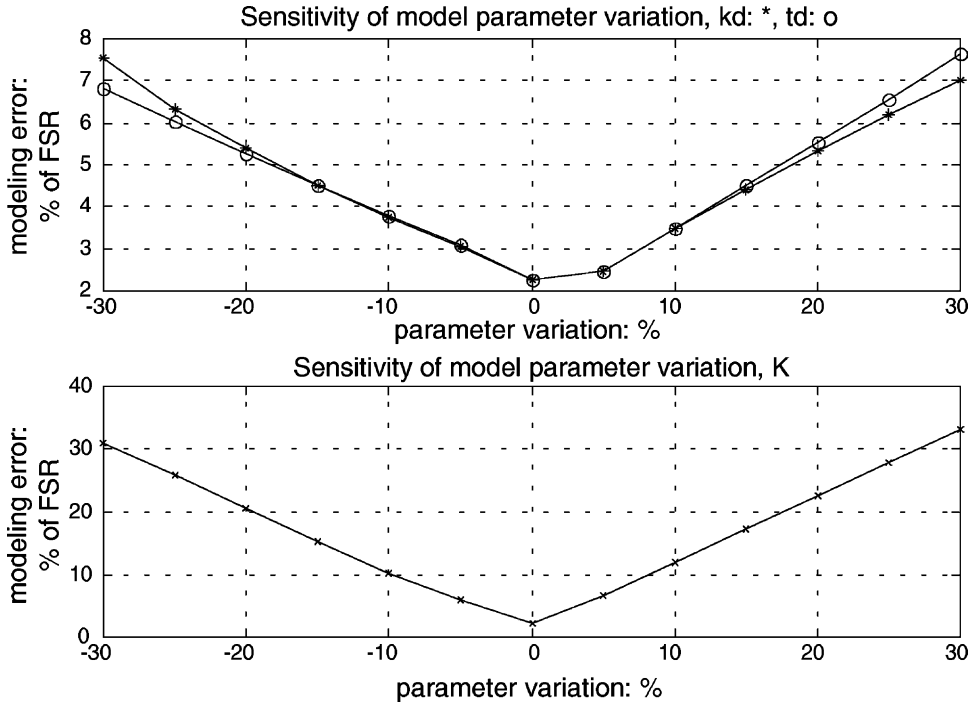

Fig. 8. Sensitivity of modeling error with the variation of model parameters; (∗) τ_d, (○) k_d, (×) K.

7. Major and minor loop simulation

When the actuator is excited by many distinct periodical waveforms, many characteristics of hysteresis are exhibited. Notably, the input waveforms in Fig. 9(a) and (b) are exponentially decreasing and increasing sinusoidal voltages with a 1 Hz frequency. The hysteresis loops converge toward the left-bottom corner. When the operating voltage decays at the midpoint of the input span, the hysteresis loops converge toward the center in Fig. 9(c). In Fig. 9(d), the hysteresis loops include minor loop trajectories. Table 3 shows the numerical results of the proposed hysteresis model, including the data concerning the minor loop behavior of the actuator, which closely approximate to the experimental data, implying that,

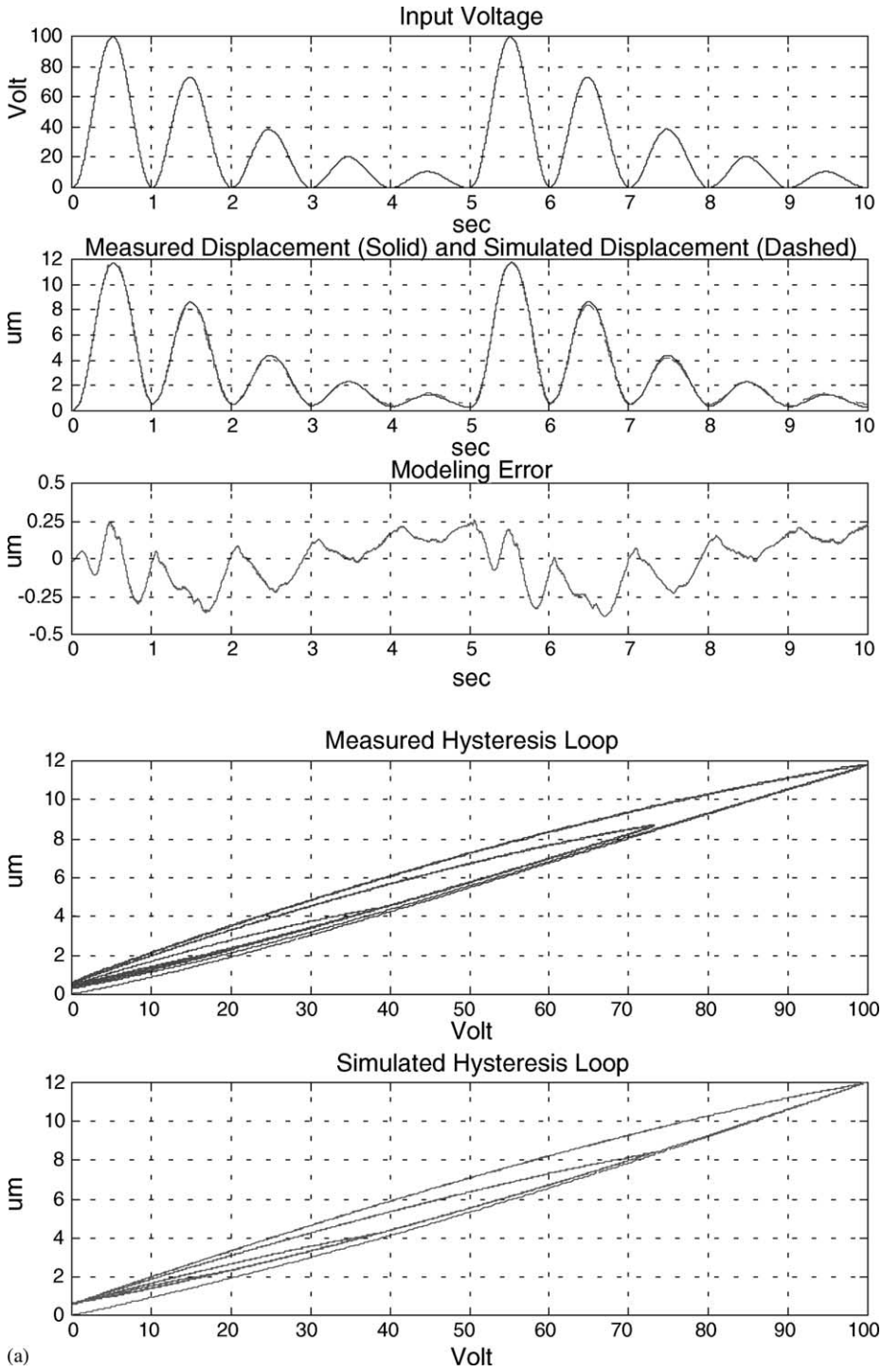

Fig. 9. Measured and simulated piezoelectric stack actuator displacement response for: 1 Hz exponential decreasing sinusoidal voltage input (a); 1 Hz exponential increasing sinusoidal voltage input (b); 1 Hz exponential decaying sinusoidal voltage input (c); 10 Hz waveform with minor loop trajectory (d).

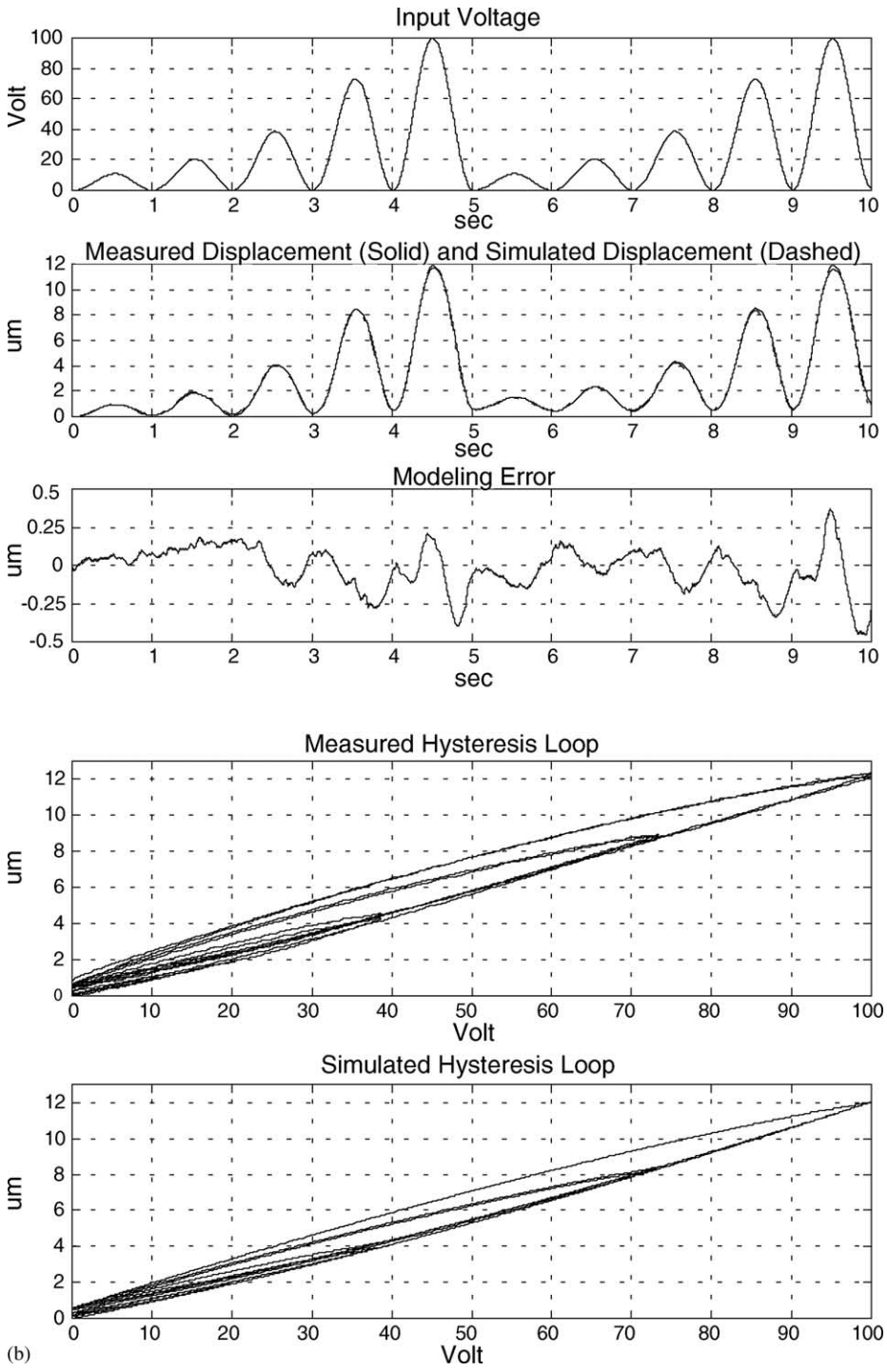

Fig. 9. (*Continued*).

for various periodical inputs, the proposed model is consistent with the actual hysteresis behavior.

The response of the piezoelectric actuator under a periodical input voltage with increasing and decreasing input spans, shows that the residual displacement near zero input voltage is not constant. That is, the most recent input span affects the magnitude of the residual displacement. When the operating waveform increases the input span of the latest cycle, the residual displacements of the actuator also increase. Similarly, residual displacements decrease when a waveform with a decreasing span is applied. This correlation arises because residual charges are stored in the piezoelectric stack. Furthermore, the piezoelectric ceramic is a capacitor that deforms linearly with supplied charge. When the periodic input voltage decreases to zero, no electrical path exists to discharge fully the previously supplied charge. In the proposed

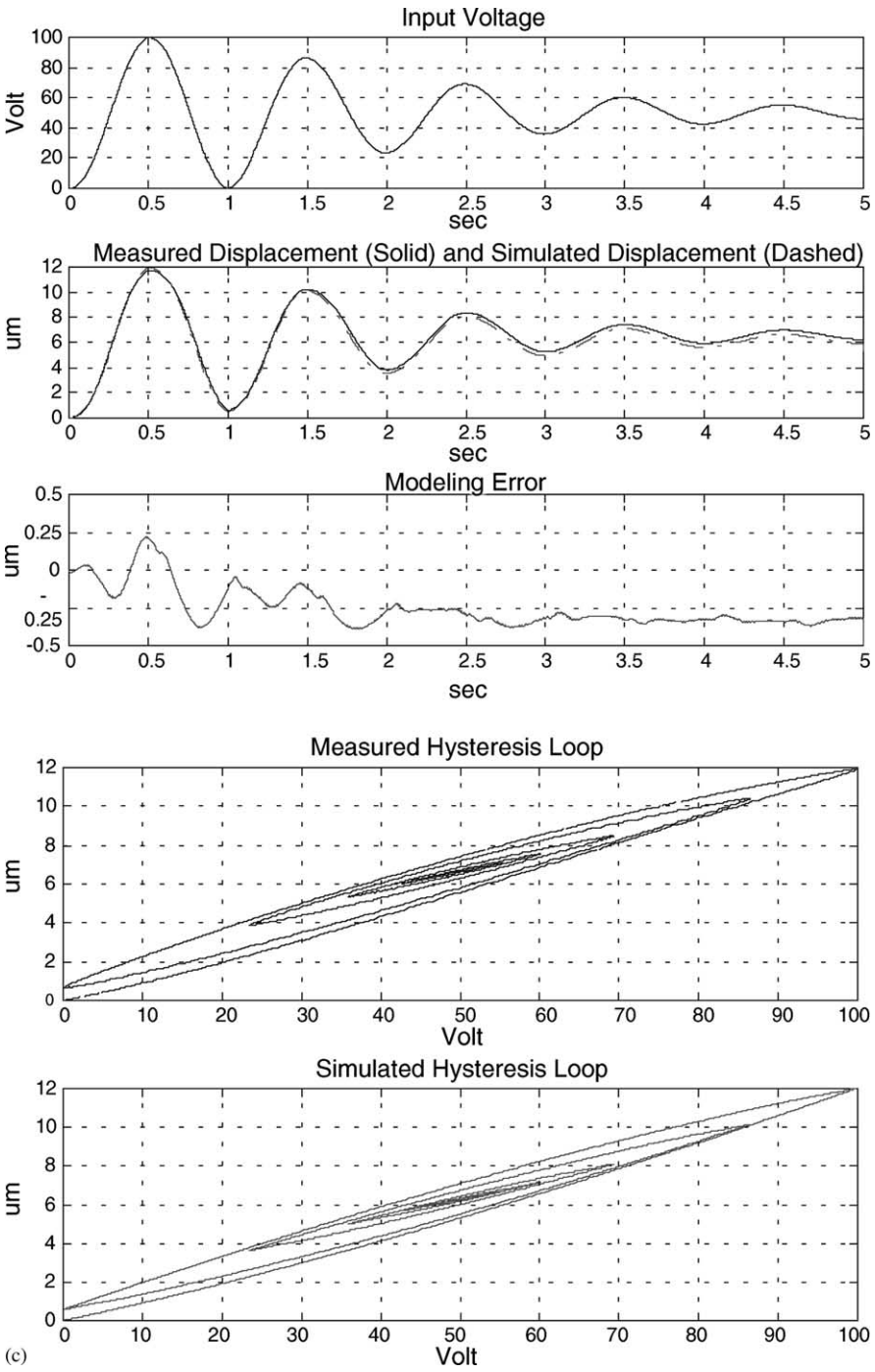

Fig. 9. (*Continued*).

hysteresis model, the simulated residual displacement increases with the input span and the most recent magnitude is maintained as the span decreases. Comparing the experimental conclusions with the numerical simulations shows that the modeling error produced by the mismatch of the residual displacement for either the increasing or the decreasing cyclic input waveform, is less than 2% of the full span displacement of the actuator, as shown in Fig. 9(a) and (b).

8. PI control with inverse model compensation

The input voltage fails to control the output displacement of the piezoelectric actuator precisely because of the hysteresis non-linearity. As shown in Fig. 10, when the tracking experiment uses a 10 Hz sinusoidal wave with a 4 μm amplitude and a 5 μm dc offset, the tracking error is between −1 and 0.5 μm. Under open-loop operation, the tracking error is around ±10% FSR. The closed-loop tracking control

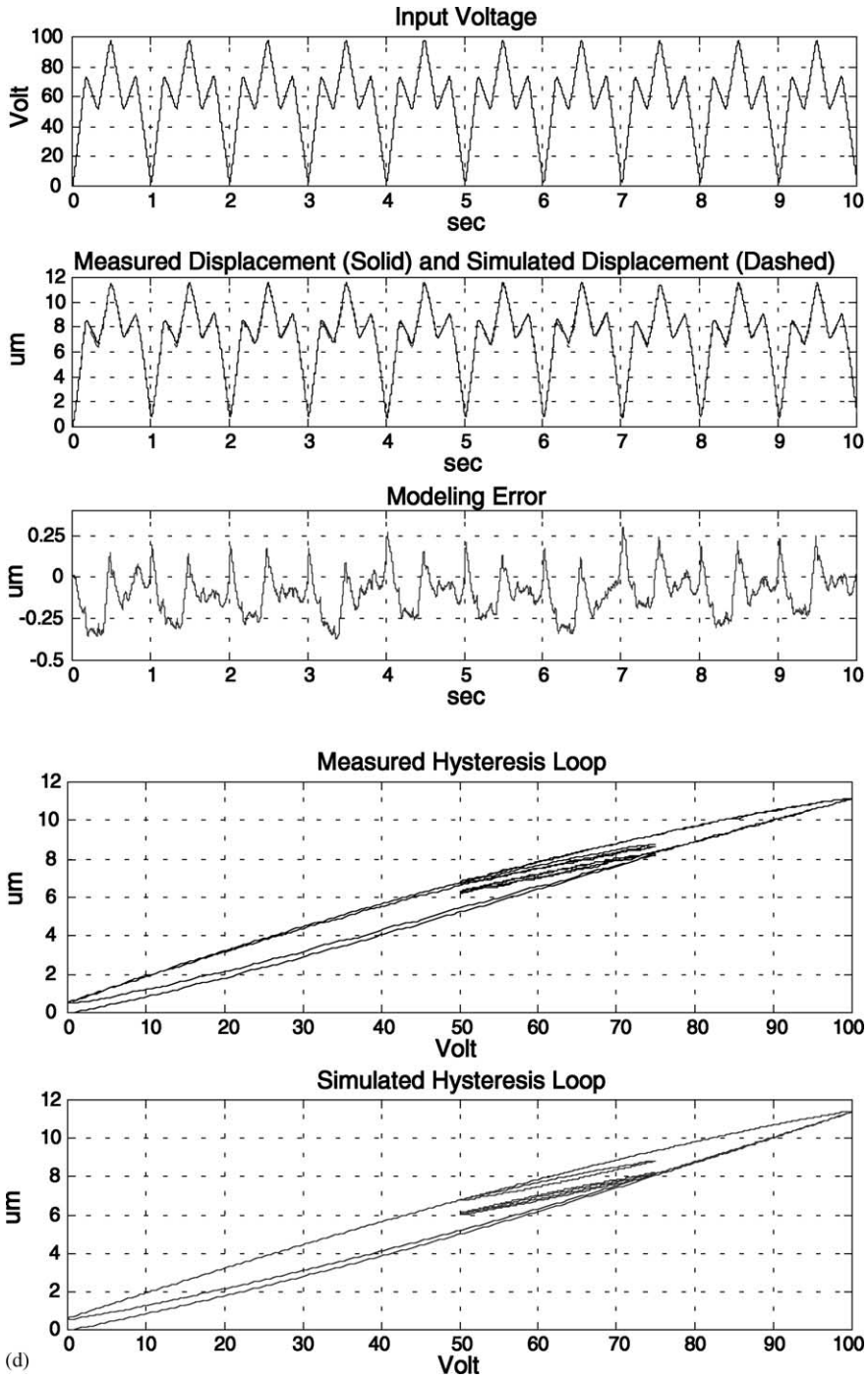

(d)

Fig. 9. (*Continued*).

scheme, such as the closed-loop PID control, may be used to suppress the tracking error between the real output and the desired output.

Compensation for hysteresis non-linearity using parallel or cascaded connections of an inverse model was demonstrated to be effective. However, the performance of such compensation schemes is determined by the accuracy of the inverse model. Geometrically, the inverse hysteresis model, which maps the output displacement onto the input voltage, should have the same mathematical form as the hysteresis model. Using the hysteresis model presented here, the inverse hysteresis model of the piezoelectric actuator can be expressed as follows:

$$V = \sum_i h_i (1 - \mathrm{e}^{-\alpha_i |L - L_{\mathrm{off}}|})(L - L_{\mathrm{off}}) + V_{\mathrm{off}}. \tag{4}$$

The definitions of variables V, V_{off}, L and L_{off} are identical to those used in the previous hysteresis model. The parameters,

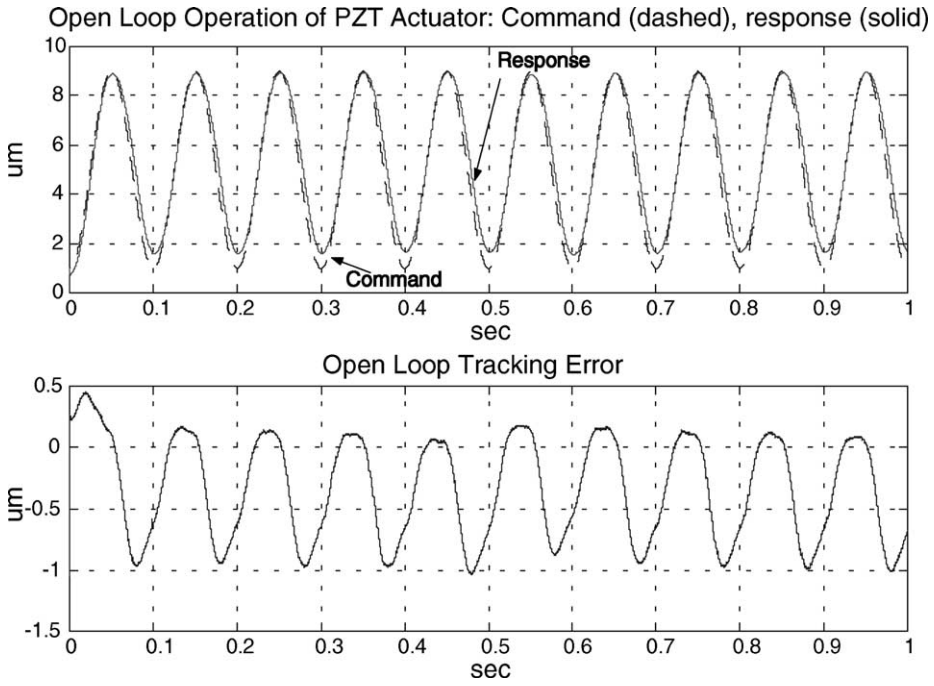

Fig. 10. Measured piezoelectric actuator response under open loop operation.

Table 4
Identified parameters of inverse hysteresis model

i	h_i (V/mm)	α_i	V_{off} (0)	$L_{\text{off}}(0)$
1[a]	−4.938	0.132	9.0	0.707
2	1.874	11.208		
3	5.515	13.837		
4	5.336	14.163		

[a] The most dominant inverse hysteresis operator in the model.

h_i and α_i, represent the gain and displacement-dependent lag of the inverse hysteresis operator, respectively. The procedure for determining the model parameters is identical to that applied to the hysteresis model. Table 4 presents the identified parameters. Notably, the first inverse hysteresis operator with the least displacement lag constant is the dominant inverse hysteresis operator. Like the hysteresis model, the inverse hysteresis model may be simplified by using only the dominant inverse hysteresis operator as follows:

$$V = (H - h_1\, \mathrm{e}^{-\alpha_1 |L - L_{\text{off}}|})(L - L_{\text{off}}) + V_{\text{off}}, \quad H = \sum_i h_i. \tag{5}$$

According to Table 4, the parameters h_i and α_i are −4.938 and 0.132 V/μm, respectively. H becomes 7.737 V/μm.

A simplified inverse hysteresis model may be employed to generate inverse model compensation for tracking control of a piezoelectric actuator. Fig. 11 presents the block diagram of PI control with inverse model feed-forward compensation. The control algorithm is expressed as follows:

$$u(i) = k_{\text{p}} e(i) + k_{\text{i}}\, \Delta T \sum_i e(i) + K^{-1} H(R(i))^{-1}, \tag{6}$$

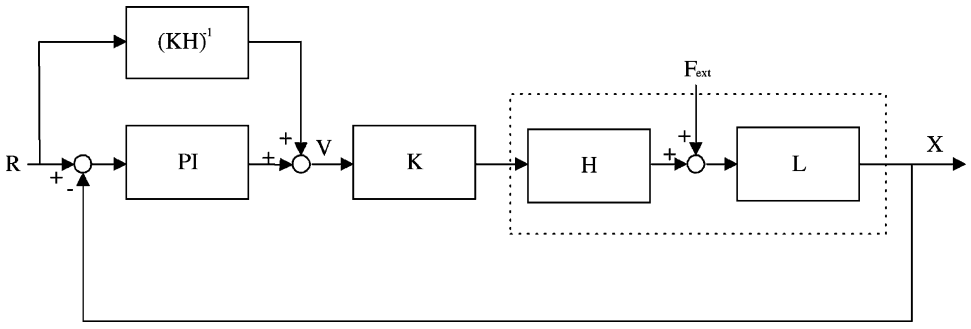

Fig. 11. The block diagram of PI control with inverse model feed-forward compensation. (K in the forward loop and the feed-forward compensation loop denotes the amplifier gain.)

where $H(\cdot)^{-1}$ represents the inverse hysteresis model, and K is the gain of the piezoelectric amplifier. The proportional gain, k_p, is 0.5, and the integral gain, k_i, is 2500.

9. Tracking performance

Fig. 12 shows the tracking performance of the compensated system. Fig. 12(a) shows that when a 10 Hz sinusoidal trajectory input is provided, the tracking error is bound within −0.01 to +0.05 μm. The error is greatly reduced from ±10% FSR obtained in the open-loop experiment to less than ±0.5% FSR. Fig. 12(b) shows that when a 100 Hz sinusoidal trajectory input is provided, the tracking error is bound within −0.1 to +0.15 μm. The error herein is reduced to under ±1.5% FSR. A bias of around 0.02 μm is evident in the error plot of Fig. 12(a). This bias, over a short measurement period, resulted from the hysteresis

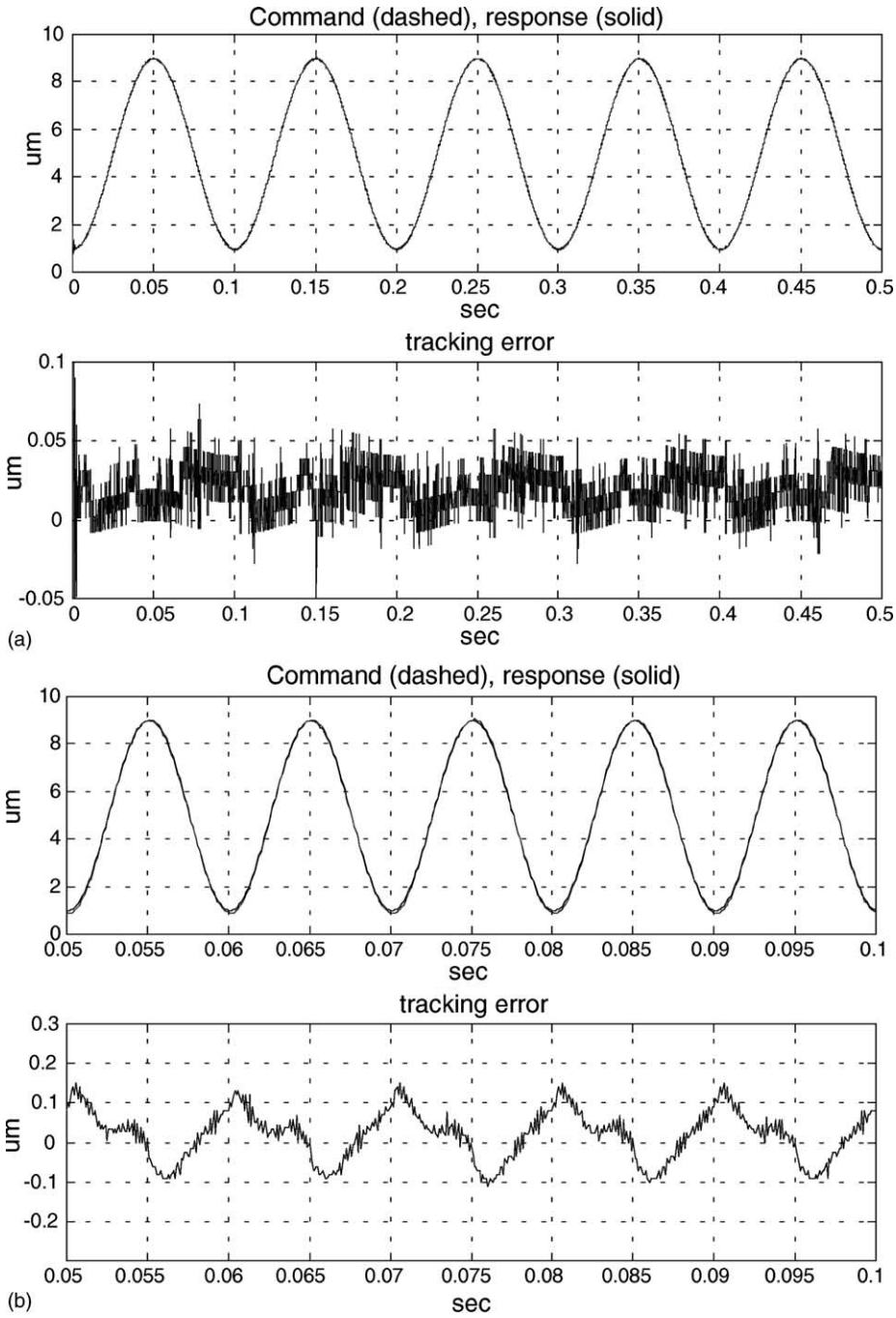

Fig. 12. PI control with inverse model feed-forward compensation of piezoelectric actuator k_p, 0.5; k_i, 2500; sampling rate, 10 kHz. (a) 10 Hz sine wave command tracking, (b) 100 Hz sine wave command tracking.

Table 5
Tracking performance of piezoelectric actuator

	Tracking error			
	100 Hz waveform		10 Hz waveform	
PI with inverse model	−0.1 to 0.15 μm	±1.5%	−0.01 to 0.05 μm	±0.5%
PI with direct feed-forward	±0.4 μm	±4%	±0.1 μm	±1%
Traditional PI	±2.5 μm	±25%	−0.1 to 0.2 μm	±2%
Open loop operation	–	–	−1 to 0.5 μm	±10%

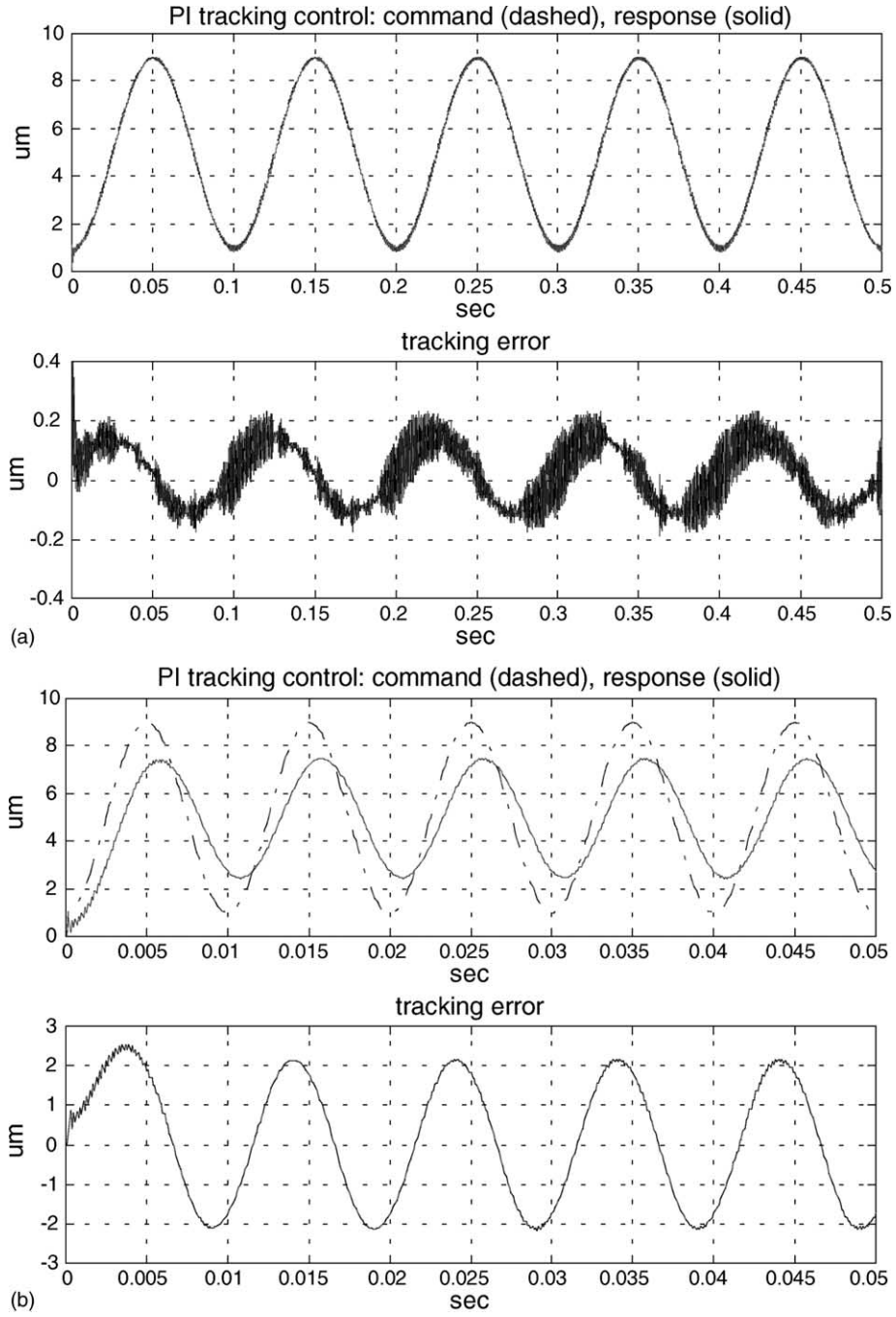

Fig. 13. PI tracking control of piezoelectric actuator (k_p, 0.75; k_i, 1875; sampling rate, 10 kHz). (a) 10 Hz sine wave command tracking, (b) 100 Hz sine wave command tracking.

non-linearity that is compensated mostly by the inverse model compensation. This un-compensated time-varying non-linearity is present, partially due to the creep (drift) of the piezoelectric material and partially due to the thermal expansion of the housing. The experimental set-up of the tracking control is identical to that in the parameter identification experiments. The control algorithm was implemented using a DSP chip TMS320C50 with a 10 kHz sampling rate.

Table 5 lists and compares the tracking performance of the piezoelectric actuator with traditional PI control, PI control with direct command feed-forward and PI control with inverse model feed-forward compensation. Both the high frequency (100 Hz) trajectory tracking and the low frequency (10 Hz) trajectory tracking experimental results are shown. In the PI control experiment, a P gain of 0.75 and an I gain of 1875 were used. Fig. 13(a) shows that when a 10 Hz sinusoidal trajectory input is provided, the tracking error is

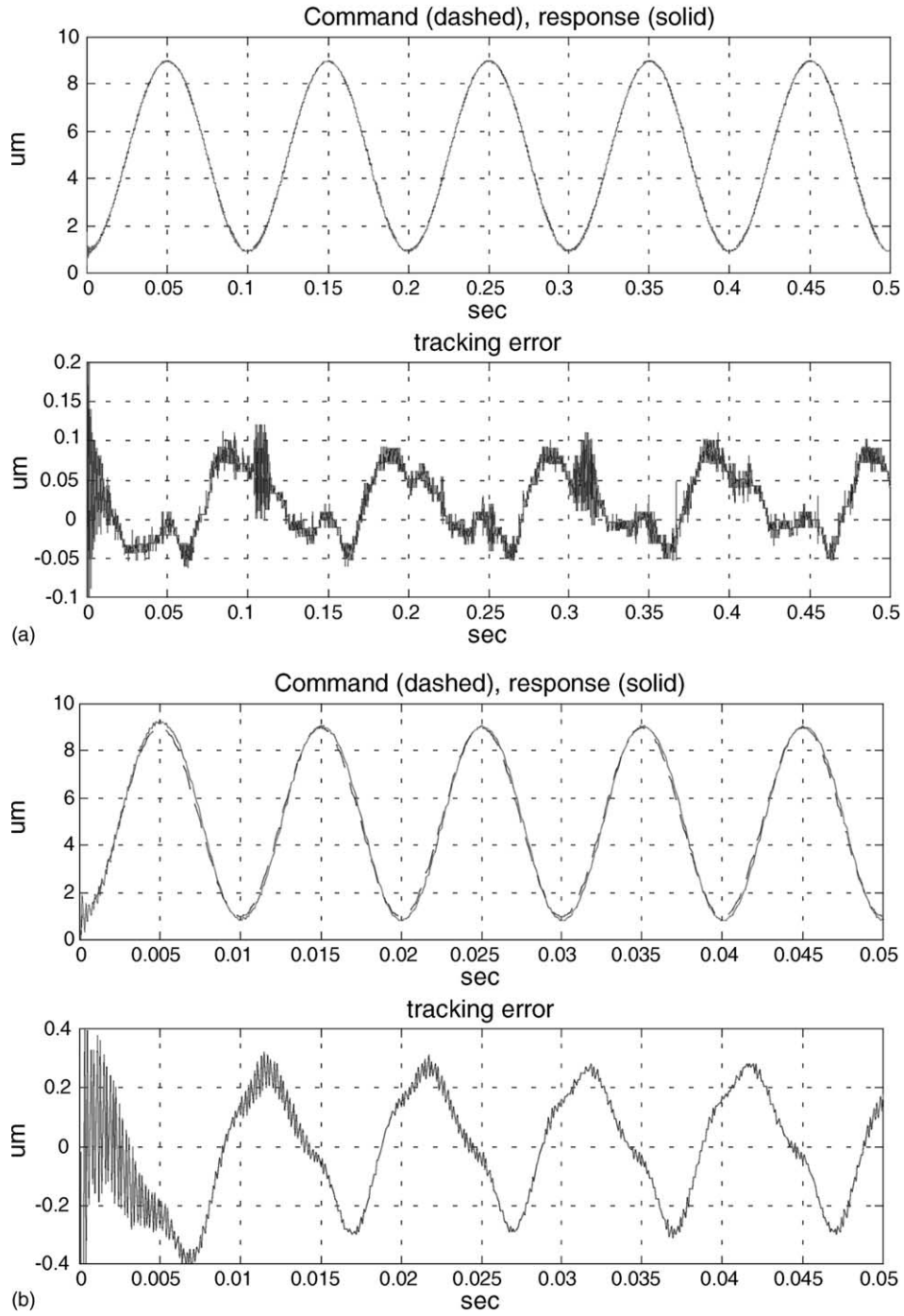

Fig. 14. PI tracking control with direct command feed-forward k_p, 0.5; k_i, 2500; sampling rate, 10 kHz. (a) 10 Hz sine wave command tracking, (b) 100 Hz sine wave command tracking.

bound within −0.1 to +0.2 μm. The error is greatly reduced from ±10% FSR in the open-loop experiment to less than ±2% FSR. Although increasing the *I* gains in a PI controller reduces the tracking error, it may also increasing the chattering in the output and render the system less stable. The conventional PI controller is limited in that its tracking error increases markedly from ±0.2 to ±2.5 μm when a faster input trajectory is tracked. Fig. 13(b) shows that the tracking error of a 100 Hz sinusoidal trajectory is around ±2.5 μm, or ±25% FSR. A signal path to feed directly the command to the plant is added to the traditional PI control, to improve the tracking performance of the piezoelectric actuator during high frequency operation. The proportional gain, k_p, is 0.5, and the integral gain, k_i, is 2500. When the piezoelectric actuator tracks 10 and 100 Hz sinusoidal waveforms, the tracking errors are approximately ±0.1 and ±0.4 μm, respectively (Fig. 14). Thus, the tracking performance of a 100 Hz sinusoidal trajectory is improved from ±25% FSR error to ±4% FSR error. For a PI control with inverse model feed-forward compensation, when the piezoelectric actuator tracks both 10 and 100 Hz sinusoidal waveforms, the tracking errors are bound between [−0.01 μm, +0.05 μm] and [−0.1 μm, +0.15 μm], respectively. PI control with inverse model feed-forward compensation significantly improves the tracking performance of a piezoelectric actuator.

10. Conclusion

This work described a hysteresis model of a piezoelectric actuator that closely matches physical reality. The model, which incorporates hysteresis operators into a parameter scheduling procedure, is flexibly adapted in a computer program and a single chip system. Herein, various periodic input waveforms were used to verify the accuracy of the new model. Moreover, the significant features of the hysteresis loop, including the minor loop trajectory and the residual displacement, are simulated correctly. The numerical simulations based upon the hysteresis model are consistent with experimental data. According to the identified parameters in the hysteresis model, selecting the dominant operator for the hysteresis behavior is easy. This model includes only the dominant hysteresis operator and thus requires little computational effort and is suitable for advanced applications. Based on the introduction of rate-independent exponential lags as the kernel of the model, the non-linear behavior of piezoelectric actuators was successfully extracted from hysteresis phenomena of a material. However, other time-dependent non-linearities of the actuators are not considered herein, including, for instance, the drift behavior of piezoceramic.

Moreover, the tracking control based on the simplified hysteresis model reduces the non-linear effect between the output displacement and the input voltage of the piezoelectric actuator. PI control with inverse model feed-forward compensation was introduced and realized in these tracking experiments. Experimental data show that the control schemes may suppress the tracking errors to within ±0.5% FSR in 10 Hz sinusoidal waveform tracking, and to within ±1.5% FSR in 100 Hz sinusoidal waveform tracking. PI control with an inverse model feed-forward compensation improves tracking performance.

The main advantages of the new hysteresis model include the following: (1) the computation of this hysteresis model is straightforward. Unlike the Preisach model, it depends on no interpolation of experimental data. (2) Fewer hysteresis operators are required to describe the non-linear behavior of hysteresis than are required by the previous models. For example, consistent modeling using a Maxwell slip requires around 10 hysteresis operators. In this proposed model, four or five hysteresis operators suffice to keep the modeling error within ±3% of FSR. (3) The inverse model is mathematically similar to the forward model, and the inverse model can be identified directly for applications of non-linear compensation. (4) The mathematical computation of this model involves exponential lag, and can be simplified to iterating a first order difference equation. It suited to real-time application. (5) A systematic procedure to identify the parameters in this model is presented. A conjugate gradient searching algorithm that minimizes the least square error between the model output and the experimental data is implemented and verified.

References

[1] Uchino K. Piezoelectric actuator and ultrasonic motors. Norwell, MA: Kluwer Academic Publishers; 1997.
[2] Jiles DC, Atherton DL. Theory of ferromagnetic hysteresis invited. J Appl Phys 1984;55(6):2115–20.
[3] Ge P, Jouaneh M. Modeling hysteresis in piezocreamic actuators. Precision Eng 1995;17:211–21.
[4] Ge P, Jouaneh M. Generalized Preisach model for hysteresis non-linearity of piezoceramic actuator. Precision Eng 1997;20:99–111.
[5] Stepanenko Y, Su CY. Intelligent control of piezoelectric actuators. In: Proceedings of 37th IEEE Conference on Decision and Control. Tampa, FL; December 1998, p. 4234–9.
[6] Goldfarb M, Celanovic N. A lumped parameter electromechanical model for describing the nonlinear behavior of piezoelectric actuators. J Dyn Syst, Measur, Control, Trans ASME 1997;119(9):478–85.
[7] Cruz-Hernandez JM, Hayward V. On the linear compensation of hysteresis. In: Proceedings of 36th IEEE Conference on Decision and Control. San Diego, CA; December 1997, p. 1956–7.
[8] Newcomb CV, Flinn I. Improving the linearity of piezoelectric ceramic actuators. Electron Lett 1982;18(11):442–4.
[9] Ge P, Jouaneh M. Tracking control of a piezoelectric actuator. IEEE Trans Control Syst Technol 1996;4(3):209–16.
[10] Choi GH, Oh JH, Choi GS. Repetitive tracking control of a coarse-fine actuator. In: Proceedings of the 1999 IEEE/ASME International Conference on Advanced Intelligent Mechatronics. Atlanta, GA; September 1999, p. 335–40.
[11] Scafer J, Janocha H. Compensation of hysteresis in solid state actuators. Sensors and Actuators A 1995;(49):97–102.
[12] The Piezo Book. Burleigh Instruments. Fishers, NY; November 1994.
[13] PZL/PZO/PZS Low Voltage Piezoelectric Device Instruction Manual. Burleigh Instruments, Fishers, NY; November 1994.
[14] PI catalog: theory and application of piezo actuators and PZT nanopositioning systems. Physik Instrument, Waldbronn, Germany; 1998.
[15] Penny J, Lindfield G. Numerical methods using Matlab. Englewood Cliffs, NJ: Prentice Hall; 1995.